Mon. Not. R. Astron. Soc. **000**, 000–000 (0000) Printed 2 February 2008 (MN LATEX style file v2.2)

Spurious contribution to CR scattering calculations

A. Shalchi[1,2], H. Yan[3] and A. Lazarian[3]
[1] *Bartol Research Institute, University of Delaware, Newark, Delaware 19716, USA*
[2] *now at: Institut für Theoretische Physik, Lehrstuhl IV: Weltraum- und Astrophysik, Ruhr-Universität Bochum, D-44780 Bochum, Germany*
[3] *Astronomy Department, University of Wisconsin, Madison, Wisconsin 53706, USA*

arXiv:astro-ph/0411074v1 2 Nov 2004

Accepted / Received

ABSTRACT
The quasilinear theory for cosmic ray propagation is a well known and widely accepted theory. In this paper, we discuss the different contributions to the pitch-angle Fokker-Planck coefficient from large and small scales for slab geometry using the damping model of dynamical turbulence. These examinations will give us a hint on the limitation range where quasilinear approximation is a good approximation.

Key words: cosmic rays – turbulence – diffusion

1 INTRODUCTION

The propagation of cosmic rays (CRs) is affected by their interaction with a magnetic field. This field is turbulent and therefore, the resonant interaction of cosmic rays with MHD turbulence has been discussed by many authors as the principal mechanism to scatter and isotropize cosmic rays (Schlickeiser 2002, Yan & Lazarian 2002). Although cosmic ray diffusion can happen while cosmic rays follow wandering magnetic fields (Jokipii 1966), the acceleration of cosmic rays requires efficient scattering. For instance, scattering of cosmic rays back into the shock is a vital component of the first order Fermi acceleration (see Longair 1997).

One important interaction between CRs and MHD turbulence is gyroresonance scattering. While the propagation of most moderate energy CRs don't sense slower time variations of turbulence, turbulence is dynamical for low energy CRs or when the parallel speed of CRs becomes comparable with Alfvén speed $v_\parallel \sim V_A$. Dynamical MHD turbulence leads to resonance broadening so that a Breit-Wigner-type function instead of a δ function should be used (Schlickeiser & Achatz 1993, Bieber et al. 1994). In this case CRs interact with a whole range of turbulence from large to small scales.

Scattering of CRs cannot happen by the magnetic wave which frequency in the particle frame is much lower than the Larmor frequency. Indeed if magnetic field changes much slower than the particle gyrorates, the quantity $v_\perp^2/B$ is preserved (Landau & Lifshitz 1957). As the result while the pitch-angle of the particle changes as the wave passes by the total change of the angle is zero.

In quasilinear theory (QLT) the assumption of unperturbed orbit results in non-conservation of the adiabatic invariant $\rho = mv_\perp^2/2B_0$. Whereas small scale contribution corresponds to the sharp resonance in magnetostatic limit, the contribution from slow large scale can be overestimated by QLT since the adiabatic invariant ought to be conserved when the electromagnetic field varies on a time scale longer than the gyroperiods of CRs Ω^{-1} (Chandran 2000, Yan & Lazarian 2003).

In QLT the turbulent field is presented in terms of Fourier modes. It is clear that the slow (compared to the particle Larmor frequency) components cannot scatter cosmic rays as the consequence of the preservation of the adiabatic invariant. However, this effect is not treated in the conventional QLT, which has been widely used to obtained a lot of results mostly within the framework of the slab model of turbulence. How reliable are those results? We attempt to answer this question within this paper.

Therefore, we will discuss the different contributions from large and small scales for the slab model of turbulence. We will give the regimes where the interaction is dominated by large and small scale contributions. This will give us a hint on the limitation range where quasilinear approximation is a good approximation. Because QLT is considered as a standard tool for the calculation of diffusion coefficients (e. g. Bieber et al. 1994, Chandran 2000, Schlickeiser 2002, Yan & Lazarian 2003) it is of great significance to explore the validity of the quasilinear approximation.

Within quasilinear theory the parallel mean free path $\lambda_\parallel$ results from the pitch-angle-cosine ($\mu = p_\parallel/p$) average of the inverse of the pitch-angle Fokker-Planck coefficient $D_{\mu\mu}$ as (Jokipii 1966, Hasselmann & Wibberenz 1968, Earl 1974)

$$\lambda_\parallel = \frac{3v}{8} \int_{-1}^{+1} d\mu \, \frac{(1-\mu^2)^2}{D_{\mu\mu}(\mu)}. \quad (1)$$

The pitch-angle Fokker-Planck coefficient is calculated from the ensemble-averaged first-order corrections to the particle

orbits in the weakly turbulent magnetic field (Hall & Sturrock 1968)

$$D_{\mu\mu}(\mu) = Re \int_0^\infty d\xi < \dot{\mu}(t)\dot{\mu}^*(t+\xi) > \quad (2)$$

and depends on the nature and statistical properties of the electromagnetic turbulence and the turbulence-carrying background medium.

In Sect.2 we derive general expressions for the pitch-angle Fokker-Planck coefficient $D_{\mu\mu}$. In Sect. 3 we compare the small scale and large scale contribution to the Fokker-Planck coefficient with each other. This results can be used to calculate the cosmic ray parallel mean free path using Eq. (1) what is done in Sect. 4.

2 THE PITCH-ANGLE FOKKER-PLANCK COEFFICIENT $D_{\mu\mu}$

The key input to the calculation of Fokker-Planck coefficients is the correlation tensor P_{ij}. It is common to assume the same temporal behaviour for all tensor components

$$P_{ij}(\vec{k},t) = P_{ij}(\vec{k},0) \cdot \Gamma(\vec{k},t) \quad (3)$$

where Γ is the dynamical correlation function. In the past several models for Γ were discussed (Schlickeiser 2002). In the current paper we use the damping model of dynamical turbulence (DT-model, Bieber et al. 1994) for slab geometry:

$$\Gamma(\vec{k},t) = \Gamma(k_\parallel,t) = e^{-\alpha|k_\parallel|v_A t}. \quad (4)$$

Here v_A is the Alfvén speed and α is a parameter which allows us to adjust the strength of dynamical effects. $\alpha = 0$ corresponds to the magnetostatic limit whereas $\alpha = 1$ corresponds to strongly dynamical turbulence.

A further important input to our calculations is the wave spectrum. For the following examinations we use a simple power spectrum without energy- and dissipation-range:

$$g(k) = \begin{cases} g_0 k^{-s} & for \quad k \geqslant k_{min} \\ 0 & for \quad k \leqslant k_{min} \end{cases} \quad (5)$$

with

$$g_0 = \frac{s-1}{8\pi}\delta B^2 k_{min}^{s-1}. \quad (6)$$

Here and in the following discussions δB is the total strength of the turbulent magnetic field and B_0 is the strength of the magnetic background field (mean field). The parameter s in Eq. (5) is the inertial-range spectral index. For a Kolmogorov-spectrum we have $s = 5/3$ which was considered by Teufel & Schlickeiser 2002 and 2003. Another choice would be $s = 3/2$ (see Cho & Lazarian 2002). Assuming this power spectrum, slab geometry and the DT-model the pitch-angle Fokker-Planck coefficient can be written as (see Teufel & Schlickeiser 2002)

$$D_{\mu\mu} = \frac{(s-1)\Omega^2(1-\mu^2)}{4k_{min}\alpha v_A}\left(\frac{\delta B}{B_0}\right)^2 \cdot k_{min}^s \times \int_{k_{min}}^\infty dk \left[\frac{k^{-s-1}}{1+\left(\frac{kv\mu-\Omega}{\alpha v_A k}\right)^2} + \frac{k^{-s-1}}{1+\left(\frac{kv\mu+\Omega}{\alpha v_A k}\right)^2}\right]. \quad (7)$$

Now we split this integral at the wavenumber $k = \epsilon k_{res}$:

$$D_{\mu\mu}^{tot} = \frac{(s-1)\Omega^2(1-\mu^2)}{4k_{min}\alpha v_A}\left(\frac{\delta B}{B_0}\right)^2 k_{min}^s \times \left\{\int_{k_{min}}^{\epsilon k_{res}} dk \left[\frac{k^{-s-1}}{1+\left(\frac{kv\mu-\Omega}{\alpha v_A k}\right)^2} + \frac{k^{-s-1}}{1+\left(\frac{kv\mu+\Omega}{\alpha v_A k}\right)^2}\right] + \int_{\epsilon k_{res}}^\infty dk \left[\frac{k^{-s-1}}{1+\left(\frac{kv\mu-\Omega}{\alpha v_A k}\right)^2} + \frac{k^{-s-1}}{1+\left(\frac{kv\mu+\Omega}{\alpha v_A k}\right)^2}\right]\right\}. \quad (8)$$

The resonant wavenumber k_{res} is defined through (see Yan & Lazarian 2002)

$$k_{res} = \frac{\Omega}{v\mu} = \frac{1}{\mu R_L} \quad (9)$$

where R_L is the gyroradius. In the first integral we have $k^{-1} \geqslant \epsilon^{-1}\mu R_L$ and the inverse wavenumber is larger than several gyroradii if $\epsilon \ll 1$. We call this case the large scales. In the second integral we have $k^{-1} \leqslant \epsilon^{-1}\mu R_L$ and the invers wavenumber is smaller than several gyroradii. We call this case the small scales. We always have

$$\frac{k_{min}}{k_{res}} = \mu R \quad (10)$$

where we used the dimensionless rigidity $R = R_L k_{min}$. In the current paper we restrict our analysis to medium rigidities ($R \ll \epsilon \ll 1, v \gg \alpha v_A$) and we have therefore

$$k_{min} \ll \epsilon \cdot k_{res}. \quad (11)$$

In this and the following equations we use $\mu = \mid \mu \mid$, $0 \leqslant \alpha \leqslant 1$ and $1 < s < 2$. With

$$D_{\mu\mu}^0 := \frac{(s-1)\Omega^2(1-\mu^2)}{4k_{min}\alpha v_A}\left(\frac{\delta B}{B_0}\right)^2 \quad (12)$$

we find

$$\frac{D_{\mu\mu}^{tot}}{D_{\mu\mu}^0} = \frac{D_{\mu\mu}^{LS}}{D_{\mu\mu}^0} + \frac{D_{\mu\mu}^{SS}}{D_{\mu\mu}^0} \quad (13)$$

where we used the large scale

$$\frac{D_{\mu\mu}^{LS}}{D_{\mu\mu}^0} = k_{min}^s \int_{k_{min}}^{\epsilon k_{res}} dk \left[\frac{k^{-s-1}}{1+\left(\frac{kv\mu-\Omega}{\alpha v_A k}\right)^2} + \frac{k^{-s-1}}{1+\left(\frac{kv\mu+\Omega}{\alpha v_A k}\right)^2}\right] \quad (14)$$

and the small scale Fokker-Planck coefficient

$$\frac{D_{\mu\mu}^{SS}}{D_{\mu\mu}^0} = k_{min}^s \int_{\epsilon k_{res}}^\infty dk \left[\frac{k^{-s-1}}{1+\left(\frac{kv\mu-\Omega}{\alpha v_A k}\right)^2} + \frac{k^{-s-1}}{1+\left(\frac{kv\mu+\Omega}{\alpha v_A k}\right)^2}\right]. \quad (15)$$

Now we split the large scale Fokker-Planck coefficient into two parts

$$\frac{D_{\mu\mu}^{LS}}{D_{\mu\mu}^0} = k_{min}^s \int_{k_{min}}^\infty dk \left[\frac{k^{-s-1}}{1+\left(\frac{kv\mu-\Omega}{\alpha v_A k}\right)^2} + \frac{k^{-s-1}}{1+\left(\frac{kv\mu+\Omega}{\alpha v_A k}\right)^2}\right] - k_{min}^s \int_{\epsilon k_{res}}^\infty dk \left[\frac{k^{-s-1}}{1+\left(\frac{kv\mu-\Omega}{\alpha v_A k}\right)^2} + \frac{k^{-s-1}}{1+\left(\frac{kv\mu+\Omega}{\alpha v_A k}\right)^2}\right] \quad (16)$$

and use the transformation $x = k_{min}/k$ in the first and $x = \epsilon k_{res}/k$ in the second integral to obtain

$$\frac{D_{\mu\mu}^{LS}}{D_{\mu\mu}^0} = A - \left(\frac{\mu R}{\epsilon}\right)^s \cdot B \quad (17)$$

where we defined the both integrals:

$$\begin{aligned} A &= \int_0^1 dx\, x^{s-1} \left[\frac{1}{1+a^2/R^2(R\mu+x)^2} \right. \\ &+ \left. \frac{1}{1+a^2/R^2(R\mu-x)^2} \right], \\ B &= \int_0^1 dx\, x^{s-1} \left[\frac{1}{1+a^2\mu^2/\epsilon^2(\epsilon+x)^2} \right. \\ &+ \left. \frac{1}{1+a^2\mu^2/\epsilon^2(\epsilon-x)^2} \right] \end{aligned} \quad (18)$$

with

$$a = \frac{v}{\alpha v_A} \gg 1. \quad (19)$$

We can also use the transformation $x = \epsilon k_{res}/k$ to simplify the small scale Fokker-Planck coefficient

$$\frac{D_{\mu\mu}^{SS}}{D_{\mu\mu}^{0}} = \left(\frac{\mu R}{\epsilon}\right)^s \cdot B. \quad (20)$$

The total Fokker-Planck coefficient is equal to

$$\frac{D_{\mu\mu}^{tot}}{D_{\mu\mu}^{0}} = A. \quad (21)$$

2.1 Analytical results

As demonstrated in Teufel & Schlickeiser 2002 the both integrals (18) can be calculated approximatelly for different cases. For medium rigidities we have $\mu R \ll \epsilon \ll 1$ and $a/R \gg 1$ and we find:

$$\begin{aligned} A(a\mu \ll 1) &\approx \frac{\pi}{\sin(\frac{\pi s}{2})}\frac{R^s}{a^s} \\ A(1 \ll a\mu) &\approx \pi\frac{R^s}{a}\mu^{s-1} \\ B(a\mu \ll \epsilon \ll 1) &\approx \frac{2}{s} \\ B(\epsilon \ll a\mu \ll 1) &\approx \frac{\pi}{\sin(\frac{\pi s}{2})}\left(\frac{\epsilon}{a\mu}\right)^s - \frac{2}{2-s}\left(\frac{\epsilon}{a\mu}\right)^2 \\ B(\epsilon \ll 1 \ll a\mu) &\approx \pi\frac{\epsilon^s}{a\mu} - \frac{2}{2-s}\left(\frac{\epsilon}{a\mu}\right)^2 \end{aligned} \quad (22)$$

With these approximations we obtain the following expressions for the total, small scale and large scale Fokker-Planck coefficient:

$$\begin{aligned} D_{\mu\mu}^{tot}(a\mu \ll 1) &\approx \frac{\pi(s-1)}{4\sin(\pi s/2)} v k_{min} \frac{\delta B^2}{B_0^2} \frac{R^{s-2}}{a^{s-1}}(1-\mu^2) \\ D_{\mu\mu}^{tot}(1 \ll a\mu) &\approx \frac{\pi(s-1)}{4} v k_{min} \frac{\delta B^2}{B_0^2} R^{s-2}\mu^{s-1}(1-\mu^2) \\ D_{\mu\mu}^{SS}(a\mu \ll \epsilon \ll 1) &\approx \frac{(s-1)}{2s} v k_{min} \frac{\delta B^2}{B_0^2} \\ &\times R^{s-2}\left(\frac{a\mu}{\epsilon}\right)^s (1-\mu^2) \\ D_{\mu\mu}^{SS}(\epsilon \ll a\mu \ll 1) &\approx \frac{\pi(s-1)}{4\sin(\pi s/2)} v k_{min} \frac{\delta B^2}{B_0^2} \frac{R^{s-2}}{a^{s-1}}(1-\mu^2) \\ D_{\mu\mu}^{SS}(\epsilon \ll 1 \ll a\mu) &\approx \frac{\pi(s-1)}{4} v k_{min} \frac{\delta B^2}{B_0^2} R^{s-2}\mu^{s-1}(1-\mu^2) \\ D_{\mu\mu}^{LS}(a\mu \ll \epsilon) &\approx \frac{\pi(s-1)}{4\sin(\pi s/2)} v k_{min} \frac{\delta B^2}{B_0^2} \frac{R^{s-2}}{a^{s-1}}(1-\mu^2) \\ D_{\mu\mu}^{LS}(\epsilon \ll a\mu) &\approx \frac{(s-1)}{2(2-s)} v k_{min} \frac{\delta B^2}{B_0^2} \\ &\times \left(\frac{\epsilon}{\mu R}\right)^{2-s} \frac{1}{a}(1-\mu^2) \end{aligned} \quad (23)$$

The magnetostatic result ($\alpha = 0$) for the total pitch-angle Fokker-Planck coefficient is

$$D_{\mu\mu}^{MS} = \frac{\pi(s-1)}{4} v k_{min} \frac{\delta B^2}{B_0^2} R^{s-2}\mu^{s-1}(1-\mu^2) \quad (24)$$

for all values of μ.

2.2 Numerical results

To test the analytical predictions we also calculated the different Fokker-Planck coefficients numerically. To calculate $D_{\mu\mu}$ or $\lambda_\parallel$ as a function of the dimensionless rigidity R we must express the ratio v_A/v through the parameter R:

$$\frac{v_A}{v} = \frac{v_A}{c}\frac{\sqrt{R_0^2+R^2}}{R} \quad (25)$$

with

$$R_0 = \frac{k_{min}}{B_0} \cdot \begin{cases} 0.511MV & \text{for } e^- \\ 938MV & \text{for } p^+ \end{cases} \quad (26)$$

Fig. 1 and 2 show the different Fokker-Planck coefficients for protons and the following set of parameters:

$$\begin{aligned} s &= 5/3 \\ k_{min} &= (0.03AU)^{-1} \\ \delta B^2/B_0^2 &= 0.2 \\ B_0 &= 4.12\ nT \\ R &= 0.001 \\ v_A &= 33.5\ km/s \\ \alpha &= 1 \end{aligned} \quad (27)$$

With these parameters we have $R_0(p^+) \approx 0.169$ and $R_0(e^-) \approx 92.1 \cdot 10^{-6}$. Fig. 1 shows the numerical calculated Fokker-Planck coefficients for $\epsilon = 1$. In this case we split the integrals at $k = k_{res}$. As expected the small scale and and large scale Fokker-Planck coefficients are approximatelly equal except for small μ where the large scale contribution is dominant. In Fig. 2 we have shown the numerical results for $\epsilon = 1/3$. Here the small scale contribution is always dominant except for small μ.

3 COMPARISON OF THE SMALL SCALE AND LARGE SCALE FOKKER-PLANCK COEFFICIENTS

In this section we calculate the ratio

$$\xi := \frac{D_{\mu\mu}^{LS}}{D_{\mu\mu}^{SS}} = \left(\frac{\epsilon}{\mu R}\right)^s \frac{A}{B} - 1 \quad (28)$$

for the cases $a\mu \ll \epsilon \ll 1$, $\epsilon \ll a\mu \ll 1$ and $\epsilon \ll 1 \ll a\mu$.

3.1 The case $a\mu \ll \epsilon \ll 1$

Here we find with Eq. (22)

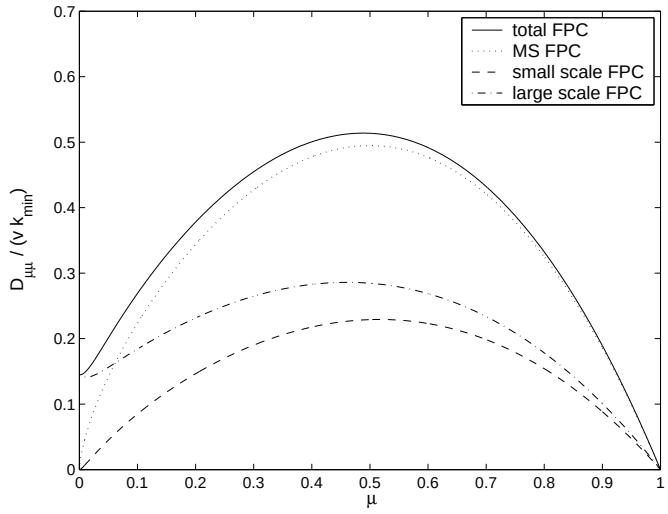

Figure 1. Numerical results for the different Fokker-Planck coefficients for protons for $\epsilon = 1$. The solid line shows the total Fokker-Planck coefficient in comparison with the magnetostatic results (dotted line), the small scale Fokker-Planck coefficient (dashed line) and the large scale Fokker-Planck coefficient (dash-dotted line).

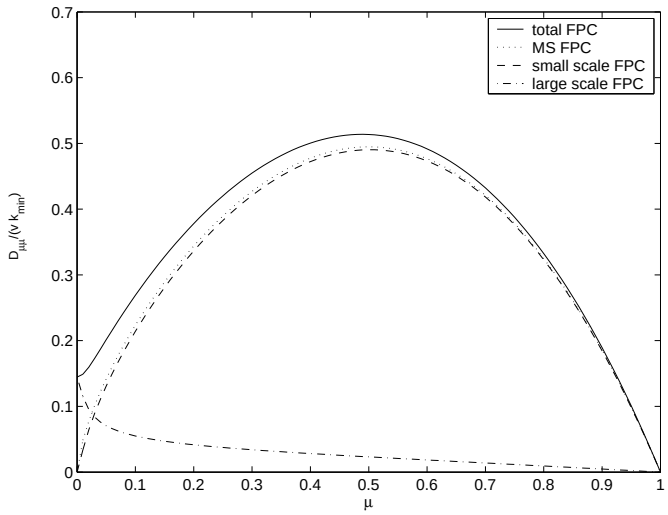

Figure 2. Numerical results for the different Fokker-Planck coefficients for protons for $\epsilon = 1/3$. The solid line shows the total Fokker-Planck coefficient in comparison with the magnetostatic results (dotted line), the small scale Fokker-Planck coefficient (dashed line) and the large scale Fokker-Planck coefficient (dash-dotted line).

$$\xi(a\mu \ll \epsilon \ll 1) = \frac{\pi s}{2\sin(\pi s/2)} \cdot \left(\frac{\epsilon}{a\mu}\right)^{s} \gg 1 \tag{29}$$

and therefore

$$D_{\mu\mu}^{LS} \gg D_{\mu\mu}^{SS}. \tag{30}$$

The last both results can also be derived directly from Eq. (23). In the case $a\mu \ll \epsilon \ll 1$ the large scale contribution is much larger then the small scale contribution.

3.2 The case $\epsilon \ll a\mu \ll 1$

In this case we have

$$\xi(\epsilon \ll a\mu \ll 1) = \frac{2\sin(\pi s/2)}{\pi(2-s)} \cdot \left(\frac{\epsilon}{a\mu}\right)^{2-s} \ll 1 \tag{31}$$

and therefore

$$D_{\mu\mu}^{LS} \ll D_{\mu\mu}^{SS}. \tag{32}$$

For $\epsilon \ll a\mu \ll 1$ the large scale contribution is much smaller then the small scale contribution.

3.3 The case $\epsilon \ll 1 \ll a\mu$

Here we find with Eq. (22) or Eq. (23)

$$\xi(\epsilon \ll 1 \ll a\mu) \approx \frac{2}{\pi(2-s)} \cdot \frac{\epsilon^{2-s}}{a\mu} \ll 1 \tag{33}$$

and therefore

$$D_{\mu\mu}^{LS} \ll D_{\mu\mu}^{SS}. \tag{34}$$

Also in the case $\epsilon \ll 1 \ll a\mu$ the large scale contribution is much smaller then the small scale contribution.

4 THE PARALLEL MEAN FREE PATH

In this section we calculate the parallel mean free path using the results for the Fokker-Planck coefficients of the last section.

4.1 The total contribution

With Eq. (23) we have

$$\begin{aligned}
\lambda_{\parallel}^{tot} &= \frac{3v}{4}\int_0^1 d\mu\, \frac{(1-\mu^2)^2}{D_{\mu\mu}^{tot}(\mu)} \\
&\approx \frac{3v}{4}\int_0^{1/a} d\mu\, \frac{(1-\mu^2)^2}{D_{\mu\mu}^{tot}(a\mu \ll 1)} \\
&+ \frac{3v}{4}\int_{1/a}^1 d\mu\, \frac{(1-\mu^2)^2}{D_{\mu\mu}^{tot}(a\mu \gg 1)}
\end{aligned} \tag{35}$$

and we obtain for the parallel mean free path

$$\begin{aligned}
\lambda_{\parallel}^{tot} &\approx \frac{3\alpha v_A v k_{min}}{\pi(s-1)\Omega^2}\frac{B_0^2}{\delta B^2}\frac{a}{R^s}\frac{2}{(2-s)(4-s)} \\
&\approx \frac{6}{\pi(s-1)(2-s)(4-s)}\frac{B_0^2}{\delta B^2}\cdot\frac{R^{2-s}}{k_{min}} \\
&\approx \lambda_{\parallel}^{MS}
\end{aligned} \tag{36}$$

which is approximatelly equal to the magnetostatic results ($\lambda_{\parallel}^{MS}$). For a Kolmogorov spectrum ($s = 5/3$) we find that the parallel mean free path is $\sim R^{1/3}$, whereas for $s = 3/2$ the parallel mean free path is $\sim R^{1/2}$.

We also find that the result for $\lambda_{\parallel}^{tot}$ is independent of the damping parameter α. Therefore we come to the conclusion that dynamical effects can be neglected if we calculate the total parallel mean free path for medium rigidities and for slab geometry. This result is in agreement with numerical calculations presented in this paper (see Fig. 1 and 2).

4.2 The small scale contribution

If we neglect the large scale contribution if we calculate the parallel mean free path we have

$$\begin{aligned}\lambda_\parallel^{SS} &= \frac{3v}{4}\int_0^1 d\mu\,\frac{(1-\mu^2)^2}{D_{\mu\mu}^{SS}(\mu)}\\ &\approx \frac{3v}{4}\int_0^{1/a} d\mu\,\frac{(1-\mu^2)^2}{D_{\mu\mu}^{SS}(a\mu\ll\epsilon\ll 1)}\\ &+ \frac{3v}{4}\int_{1/a}^{1/\epsilon} d\mu\,\frac{(1-\mu^2)^2}{D_{\mu\mu}^{SS}(\epsilon\ll a\mu\ll 1)}\\ &+ \frac{3v}{4}\int_{1/\epsilon}^{1} d\mu\,\frac{(1-\mu^2)^2}{D_{\mu\mu}^{SS}(\epsilon\ll 1\ll a\mu)} \qquad (37)\end{aligned}$$

and together with Eq. (23) we find for the parallel mean free path

$$\lambda_\parallel^{SS}\sim\int_0^{1/a} d\mu\,\frac{1-\mu^2}{\mu^s}+...\to\infty. \qquad (38)$$

If we neglect the large scale contribution the parallel mean free path goes to infinity. This result comes from very small values of μ. It should be noted that in this regime QLT is no longer valid because for $\mu\to 0$ nonlinear effects are essential (see Shalchi 2005). If we would use a more accurate, nonlinear theory instead of QLT, the problem of the infinitely large parallel mean free path (Eq. (38)) should vanish.

4.3 The large scale contribution

If we neglect the small scale contribution if we calculate the parallel mean free path we have

$$\begin{aligned}\lambda_\parallel^{LS} &= \frac{3v}{4}\int_0^1 d\mu\,\frac{(1-\mu^2)^2}{D_{\mu\mu}^{LS}(\mu)}\\ &\approx \frac{3v}{4}\int_0^{\epsilon/a} d\mu\,\frac{(1-\mu^2)^2}{D_{\mu\mu}^{LS}(a\mu\ll\epsilon)}\\ &+ \frac{3v}{4}\int_{\epsilon/a}^{1} d\mu\,\frac{(1-\mu^2)^2}{D_{\mu\mu}^{LS}(\epsilon\ll a\mu)}. \qquad (39)\end{aligned}$$

With Eq. (23) we obtain for the parallel mean free path

$$\lambda_\parallel^{LS}\approx\frac{3(2-s)}{(s-1)(3-s)(5-s)}\frac{B_0^2}{\delta B^2}\cdot\frac{R^{2-s}}{k_{min}}\frac{a}{\epsilon^{2-s}}. \qquad (40)$$

In this case the parallel mean free path is larger than the magnetostatic result. This would be the case when the turbulence is damped at a scale larger than the resonant scale.

5 DISCUSSIONS AND SUMMARY

In the current paper we calculated the pitch-angle Fokker-Planck coefficient and the parallel mean free path using QLT. Our intension was to find out how important dynamical effects are for pure slab geometry and for medium rigidities and whether the small scale or the large scale contribution controlls the total Fokker-Planck coefficient and the parallel mean free path.

If we consider Eq. (36) we come to the conclusion that we can neclect dynamical effects if we calculate the parallel mean free path for medium rigidities. The situation would be different if we would consider small rigidities and if we would use a power spectrum with dissipation range. This was considered in Teufel & Schlickeiser 2002 and 2003 for pure slab geometry and in Shalchi & Schlickeiser 2003 for pure 2D and composite slab/2D geometry.

In the current paper we compared the different contributions to the Fokker-Planck coefficient. We find that for $a\mu\ll\epsilon$ the large scale contribution controlls the Fokker-Planck coefficient whereas for $\epsilon\ll a\mu$ the small scale contribution is dominant. Thus for slab model turbulence quasilinear approximation is a good approximation except for CRs with pitch angle close to 90^o. In this regime ($\mu\approx 0$) nonlinear effects can no longer be neglected (see Shalchi 2005). Because of the results of the current paper we come to the conclusion that previous calculations done in the quasilinear limit and for slab geometry are valid. In non-slab models (e.g. the composite slab/2D model of Bieber et al. 1994) however, nonlinear effects always play a significant role, because perpendicular diffusion itself can have a strong influence on pitch-angle scattering (see Shalchi et al. 2004).

ACKNOWLEDGMENTS

This work was supported by the NSF grant AST-0307869 ATM-0312282 and the NSF Center for Magnetic Self Organization in Laboratory and Astrophysical Plasmas. This research was also supported by the National Science Foundation under grant ATM-0000315. This work is the result of a collaboration between the University of Bochum, Theoretische Physik IV and the University of Wisconsin-Madison, Department of Astronomy.

REFERENCES

Bieber, J. W., Matthaeus, W. H., Smith, C. W., et al. 1994, ApJ 420, 294
Chandran, B., 2000, Phys. Rev. Lett., 85, 22
Cho, J. & Lazarian, A., 2002, PhrL 88, 24
Earl, J. A., 1974, ApJ 193, 231
Hall, D. E. & Sturrock, P. A., 1967, Phys. Fluids 10, 2620
Hasselmann, K. & Wibberenz, G., 1968, Z. Geophys. 34, 353
Jokipii, J. R., 1966, ApJ 146, 480
Landau, L. D. & Lifshitz, E. M., Butterworth-Heinemann, 1957
Longair, M. S., Cambridge University Press, Cambridge, 1997
Schlickeiser, R. & Achatz U., 1993, J. Plasma Phys. 49, 63
Schlickeiser, R., Springer-Verlag, Berlin, 2002
Shalchi, A. & Schlickeiser, R., 2004, ApJ, 604, 861
Shalchi, A., Bieber, J. W. & Matthaeus, W. H. & G. Qin, 2004, ApJ, accepted
Shalchi, A., 2005, submitted
Teufel, A. & Schlickeiser, R., 2002, A&A, 393, 703
Teufel, A. & Schlickeiser, R., 2003, A&A, 397, 15
Yan, H. & Lazarian, A., 2002, Phys. Rev. Lett., 89, 28
Yan, H. & Lazarian, A., 2003, ApJ, 592, 33L